Available online at www.sciencedirect.com
SCIENCE DIRECT®
Bioorganic & Medicinal Chemistry 12 (2004) 5753–5766
Bioorganic & Medicinal Chemistry

ATP-phosphopeptide conjugates as inhibitors of Src tyrosine kinases

Nguyen-Hai Nam,[a] Sungsoo Lee,[b] Guofeng Ye,[a] Gongqin Sun[b] and Keykavous Parang[a,*]

[a]*Department of Biomedical and Pharmaceutical Sciences, College of Pharmacy, The University of Rhode Island, 41 Lower College Road, Kingston, Rhode Island 02881, USA*
[b]*Department of Cell and Molecular Biology, The University of Rhode Island, Kingston, Rhode Island 02881, USA*

Received 6 August 2004; revised 27 August 2004; accepted 27 August 2004
Available online 18 September 2004

Abstract—A number of Src SH2 domain inhibitors enhance the kinase catalytic activity by switching the closed inactive to the open active conformation. ATP-phosphopeptide conjugates were designed and synthesized as Src tyrosine kinase inhibitors based on a tetrapeptide sequence pTyr-Glu-Glu-Ile (pYEEI) and ATP to block the SH2 domain signaling and substrate phosphorylation by ATP, respectively. In general, ATP-phosphopeptide conjugates with optimal linkers such as compounds **5** and **7** (K_i = 1.7–2.6 μM) showed higher binding affinities to the ATP-binding site relative to the other ATP-phosphopeptide conjugates having short or long linkers, **1**–**4** and **6**, (K_i = 10.1–16.1 μM) and ATP (K_m = 74 μM). These ATP-phosphopeptide conjugates may serve as novel templates for designing protein tyrosine kinase inhibitors to block SH2 mediated protein–protein interactions and to counter the activation of enzyme that resulted from the SH2 inhibition.

1. Introduction

Protein tyrosine kinases (PTKs) are enzymes that catalyze phosphorylation of tyrosine in many proteins by the transfer of the γ-phosphoryl group from ATP. PTKs are involved in several cellular responds such as mitogenesis,[1] differentiation,[2] migration,[3] and survival.[4] A number of agents have been approved by the United States Food and Drug Administration (FDA) as PTK inhibitors including small molecules such as STI-571 (Gleevec™) against Abl,[5] ZD-1839 (Iressa™) against intracellular domain of EGFR,[6] and monoclonal antibodies such as Herceptin (Trastuzumab™) against HER2[7] and Bevacizumab (Avastin™) against VEGFR.[8]

The Src family of protein tyrosine kinases, Src, Yes, Lck, Fyn, Lyn, Fgr, Hck, Blk, and Yrk, are cytoplasmic nonreceptor tyrosine kinases (NRTKs).[9] Enhanced Src tyrosine kinases activity has been directly linked to T-cell activation, mitogenesis, differentiation, cell transformation, and oncogenesis.[10] Src kinases are important targets for drug discovery in several diseases such as cancer, bone related diseases, and autoimmune diseases.[10–16] For example, Src has been associated with several different cancers including colon[17] and breast[18] cancers for which transformed phenotypes have been correlated with Src mutations and/or over-expression[9–11] of Src tyrosine kinase activities.[19] Src has also been implicated in the development of osteoporosis and inflammation-mediated bone loss.[20–22] Lck is a positive activator in T-cell signaling, and its activation is involved in autoimmune diseases such as rheumatoid arthritis.[12]

Src family kinases share common structural motifs that determine their cellular and catalytic activity. The homologous domains include: (i) the fatty acid acylation domain, which targets the kinases to the plasma membrane, (ii) the Src homology 3 (SH3), Src homology 2 (SH2) domains, which facilitate protein–protein interactions, (iii) the kinase domain, and (iv) the C-terminal regulatory domain. The conserved ~260 amino acid kinase domain architecture folds into a two-lobe structure, a smaller N-terminal lobe (NT lobe) that is associated with ATP binding, and a larger C-terminal lobe (CT lobe) that is associated mainly with peptide/protein binding.[23]

Keywords: Src tyrosine kinases; Src SH2 domain; pYEEI; Inhibitors.
* Corresponding author. Tel.: +1 401 874 4471; fax: +1 401 874 5048; e-mail: kparang@uri.edu

0968-0896/$ - see front matter © 2004 Elsevier Ltd. All rights reserved.
doi:10.1016/j.bmc.2004.08.043

SH2 domains are protein domains of ~100 amino acids that recognize and bind specifically to tyrosyl-phosphorylated sequences located on proteins involved in signal transduction[23,24] in response to extracellular signals.[24–26] The SH2 domain controls the range of proteins interacting with the Src family kinases such as FAK, p130^{cas}, p85, PI3K, and p68^{sam}.[27–30] The phosphotyrosyl group (pTyr) of phosphoproteins binds in a positively charged phosphotyrosine binding pocket of SH2 domain. Ligands having the ability to disrupt cellular signal transduction pathways by antagonizing SH2 domain-dependent protein–protein interactions provide possible therapeutic agents.[31–36] Tetrapeptide pTyr-Glu-Glu-Ile (pYEEI) has high affinity (K_d = 100 nM) for the SH2 domain of Src tyrosine kinase[31] that makes it an attractive lead structure for the rational design of agents to compete with the SH2 domain's natural ligands.

Common strategies for designing Src inhibitors are to target the conserved ATP-binding site and the SH2 domain. High-affinity ligands targeting either ATP-binding site or the Src SH2 domain have been developed.[24,37] Designing inhibitors against ATP-binding site is a significant challenge, due to the presence of a large number of protein kinases that show a conserved ATP-binding site. Although selective inhibitors competitive with ATP have been identified[38] for specific protein kinases, the process is labor intensive due to the high structural homology between protein kinase active site regions.[39–44] Gleevec™ is an Abl Tyr kinase inhibitor, was approved by FDA for the treatment of chronic myelogenous leukemia.[45,46] In addition to Abl, three other kinases have been reported to be inhibited by Gleevec: the Abl-homologue Arg, stem cell factor receptor (c-Kit), and PDGF receptor.[47,48] Iressa™, a potent EGFR kinase inhibitor, is in the clinic for the treatment of nonsmall cell lung carcinoma.[49] Reported pulmonary toxicity has complicated the use of this drug in several patients.[50] This lack of specificity highlights one disadvantage of ATP analogs as PTK inhibitors.

The design of SH2 inhibitors has focused on peptidomimetic modifications of cognate peptide sequences. SH2 domain-directed pTyr mimetics,[51–59] carboxylic acid-based pTyr mimetics,[60–64] uncharged pTyr mimetics,[65] and conformationally constrained peptides.[66] Although significant efforts have been made on the development of SH2 domain inhibitors to inhibit SH2 mediated signaling event, much less attention has been paid to the outcome of this inhibition and kinase activation. Tyr527 is located in the C-terminal tail of Src and, when phosphorylated by another protein kinase called C-terminal Src kinase (Csk), binds to the SH2 domain of Src,[23,67] leads to the kinase inactivation, and locks the c-Src molecule in an inhibited closed conformation. C-terminal tail dephosphorylation or competitive binding of optimal SH2 domain ligands, allows the kinase domain to switch from a closed to an open conformation.[23] The kinase reactivation by different pTyr-containing peptides related to pYEEI known to bind the SH2 domain of Src has been demonstrated.[68–71] Src is known to be activated by dual SH3/SH2 interactions with sequences in the focal adhesion kinase FAK[72] and Sin.[73] Upon the activation of the enzyme, a dramatic structural reorientation between the SH2 domain and the active site regions will occur positioning the SH2 domain closer to the active site region.[67] Designing inhibitors against Src SH2 domain-mediated protein–protein interactions has been complicated since several of these inhibitors could enhance the kinase catalytic activity[68–71] by switching the closed inactive to the open active conformation by disrupting the intramolecular interactions between the Tyr[527]-phosphorylated C-terminal tail and the SH2 domain.[68–73] Such events might lead to side effects that would prevent SH2 inhibitors to be developed as a drug.

We have previously shown that substitution on γ-phosphate of ATP with different moieties does not prevent or greatly reduce the ability of ATP for binding to ATP-binding site of Csk.[74] This allowed to hook up ATP to peptide substrate to create bivalent inhibitors. Additionally, short and long chain substitution on N-terminal of tetrapeptide pYEEI with aliphatic alkyl derivatives did not cause any significant loss in binding affinity to the Src SH2 domain.[65] *N*-substituted derivatives of pYEEI were selected for conjugation with ATP to synthesize a number of ATP-pYEEI conjugates (**1**–**7**, Fig. 1) and to examine their inhibition pattern (potency and kinetics) against Src kinases. Several strategies used for designing bivalent inhibitors of protein kinases have been reviewed;[75] none of these approaches target SH2 domain and ATP-binding site of kinase domain. We investigated by linking ATP with a phosphopeptide, whether it is possible to convert ATP substrate into a high-affinity inhibitor for Src kinases through exploiting the SH2 and ATP molecular recognition motifs and/or the kinase activation associated with SH2 inhibition can be reduced.

To generate an effective bivalent ligand, it was necessary to connect the ATP and phosphopeptide binding modules with a linker that spans the distance between the binding sites on the active form of kinase (Fig. 2). This was found to be particularly important in exploiting the knowledge gained from previous analysis of the phosphoryl transfer transition state.[76] Since the crystal structure of active form of Src kinase is not available, alkyl chains of varying length of aminoacyl derivatives [–CO(A)NH–] were utilized as linkers to understand the relationship between linker length and inhibitory potency. Src and Lck were selected as tyrosine kinases as the target enzymes because phosphopeptide substrates (pYEEI) for these enzymes have well characterized kinetically.

To understand the role and importance of ATP moiety in the whole inhibition effect, an adenosine analog (**8**) and a control pYEEI-adenosine conjugate (**9**), in which the ATP was replaced with 4-(sulfamoyl)-benzoyladenosine (SBA), an uncharged adenosine derivative, were synthesized (Fig. 3).

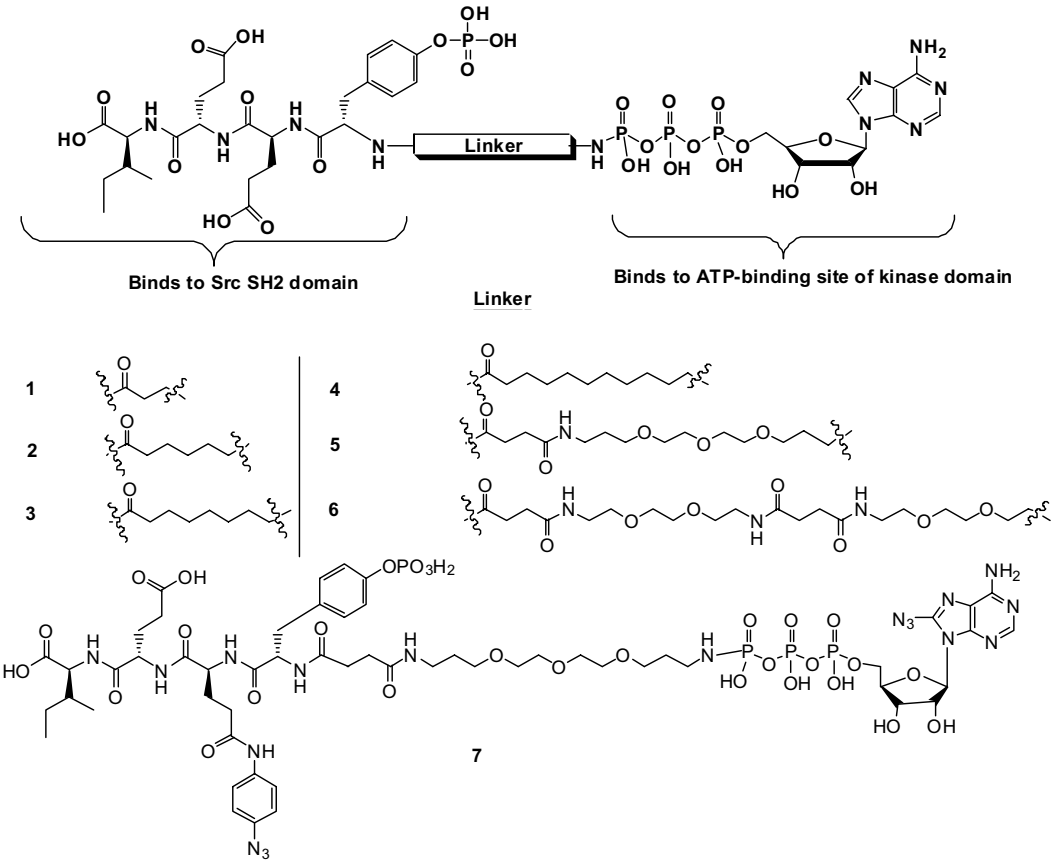

Figure 1. Synthesized ATP-phosphopeptide conjugates (**1**–**7**) as Src kinase inhibitors targeting the Src SH2 domain and ATP-binding site.

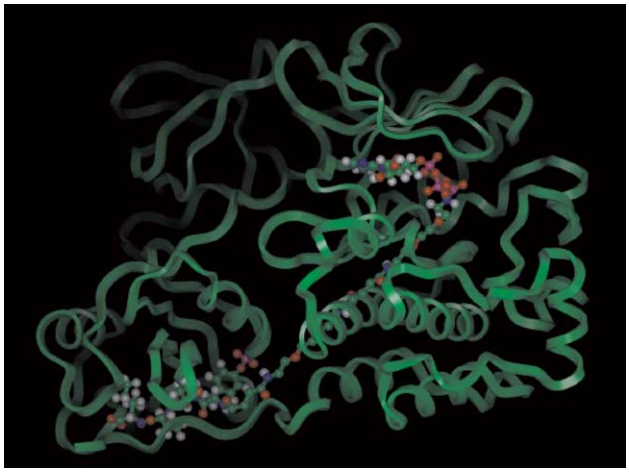

Figure 2. Simulated binding mode of an ATP-phosphopeptide conjugate (ball and stick model) with inactive Src (PDB 2SRC, ribbon). The carbon skeleton of ATP conjugate is green, hydrogens are white, oxygen atoms are red, nitrogens are blue, and phosphorous atoms are cyan. The Figure is drawn using the Accelrys visualization system.

2. Results and discussion

2.1. Chemistry

The synthesis of ATP-phosphopeptide conjugates (**1**–**6**) were carried out as shown in Scheme 1. The protected SH2-directed phosphopeptides were synthesized on Fmoc-Ile-Wang-resin, utilizing a standard Fmoc (*N*-(9-fluorenyl)methoxycarbonyl) solid-phase protocol in the presence of HBTU, *N*-methylmorpholine (NMM), and piperidine to afford **10**. The phosphopeptide-attached resin **10** underwent coupling reaction with *N*-Fmoc protected amino acids (HOOC–(A)–NHFmoc; A = flexible alkyl groups) or succinic anhydride followed by HOOC–(A)–NHFmoc to yield **11**. The phosphopeptide-attached linkers (**12**–**17**) were cleaved from the resin **11** and deblocked with trifluoroacetic acid (TFA), and then purified by preparative reversed-phase high performance liquid chromatography (HPLC) on a C18 column, utilizing a linear gradient of CH_3CN/H_2O containing 0.1% TFA. Final conjugation with adenosine 5′-triphosphate sodium salt (ATP) was carried out in the presence of *N*-cyclohexyl-*N*′-(2-morpholinoethyl)carbodiimide methyl-*p*-toluene sulfonate (CMD-CDI) at pH 7 to yield **1**–**6**. High-resolution electrospray mass spectrometry was used to confirm the identity of the final products.

Scheme 2 displays the synthesis of the diazido ATP-phosphopeptide conjugate **7**. Fmoc solid-phase peptide synthesis on Ile-Wang resin was carried out using Fmoc-Glu(*t*Bu)-OH and Fmoc-Glu(Ph*i*Pr)-OH as protected amino acids to yield **18**. The deprotection of Ph*i*Pr group on the γ-carboxylic moiety of the β-glutamic acid with TFA/DCM/TIPS followed by reaction with *p*-azidoaniline and NMM in dark condition, and subsequent coupling reactions with Fmoc-Tyr(PO_3H_2)-OH,

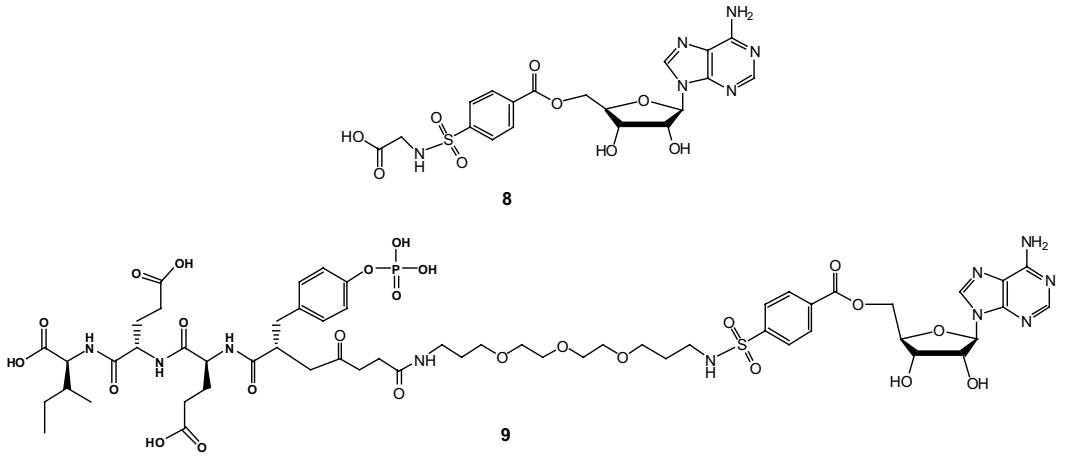

Figure 3. Chemical structures for 4-(carboxymethylsulfamoyl)benzoyladenosine (**8**) and synthesized 4-(sulfamoyl)benzoyladenosine-pYEEI (SBA-pYEEI) conjugate (**9**) as compounds with no binding affinity to ATP-binding site.

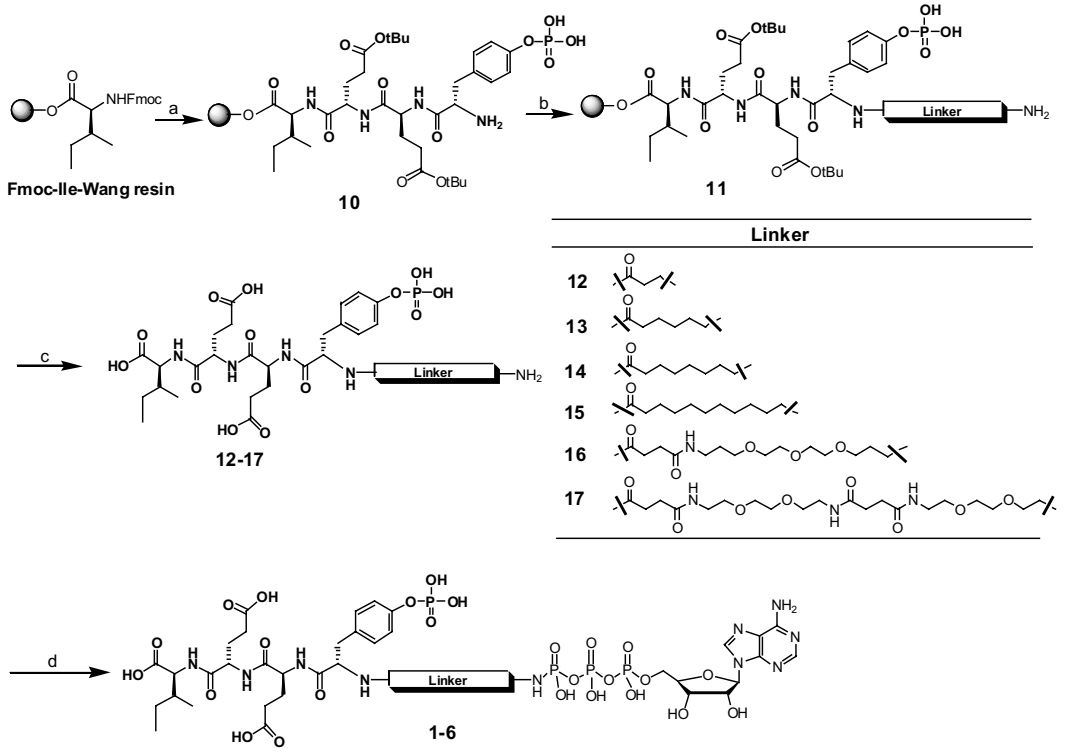

Scheme 1. General synthetic strategy for the preparation of ATP-phosphopeptide conjugates (**1**–**6**). Reagents and conditions: (a) Fmoc-peptide chemistry: Fmoc-AA-OH, HBTU, NMM, piperidine, DMF; (b) (i) FmocNH(A)COOH, (ii) piperidine/DMF (1:4) or (i) succinic anhydride, NMM, DMF, (ii) 3,6,9-trioxa-1,13-diamine, HBTU, NMM, DMF or (i) succinic anhydride, NMM, DMF, (ii) 1,8-diamino-3,6-dioxaoactane, HBTU, NMM, DMF, (iii) succinic anhydride, NMM, DMF, (iv) 1,8-diamino-3,6-dioxaoactane, HBTU, NMM, DMF; (c) TFA, anisole, water; (d) ATP, CMD-CDI, water, pH = 7.

succinic anhydride, and 4,7,10-trioxa-1,13-tridecanediamine, respectively, afforded **19**. Cleavage of **19** using TFA furnished peptide **20** that was reacted with 8-azidoadenosine 5′-triphosphate disodium salt (8-Azido-ATP) in the presence of CMD-CDI at pH7 to yield the diazido ATP-phosphopeptide conjugate **7**.

Scheme 3 shows the procedure for the preparation of 4-(carboxymethyl-sulfamoyl)-benzoyladenosine (**8**). Fmoc-Gly-Wang resin was deprotected with piperidine and reacted with 4-(chlorosulfonyl)benzoic acid to afford the resin **21**. The reaction of 2′,3′-*O*-isopropylideneadenosine with the resin **21** in the presence of DCC and DMAP gave the resin **22** that upon cleavage with TFA afforded benzoyladenosine derivative **8**.

Scheme 4 demonstrates the preparation of SBA-linker-pYEEI derivative (**9**). The resin-bound pYEEI peptide

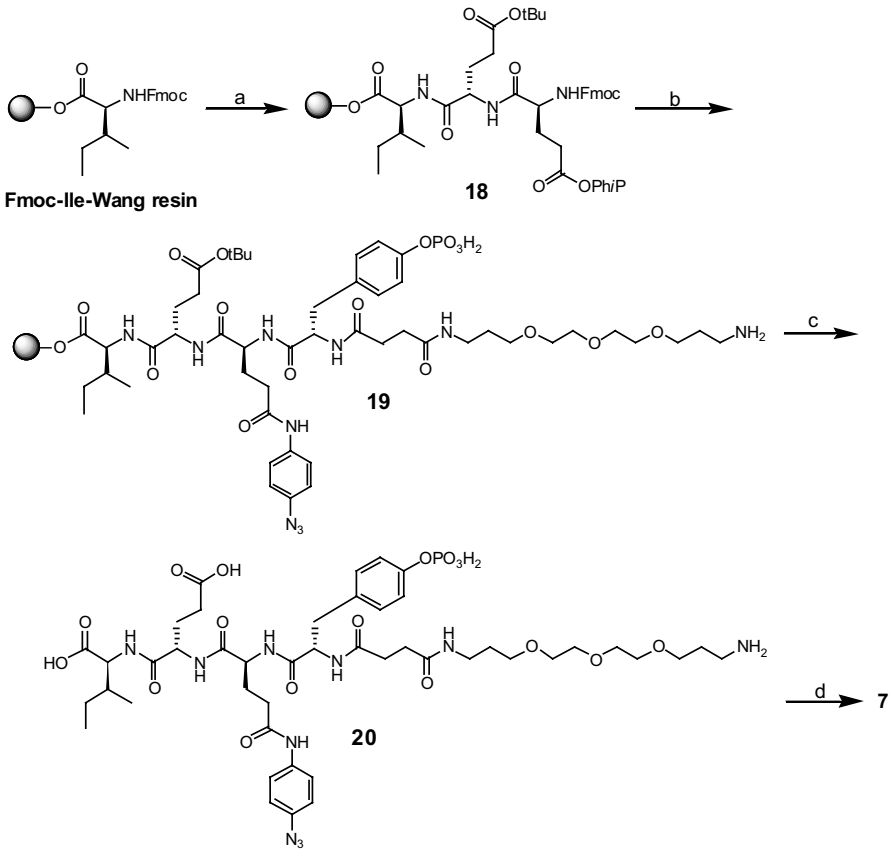

Scheme 2. Synthesis of diazido ATP-phosphopeptide conjugate **7**. Reagents and conditions: (a) Fmoc-peptide chemistry; (b) (i) TFA/DCM/TIPS (1:94:5), (ii) *p*-azidoaniline, HBTU, NMM, DMF, (iii) piperidine 20%/DMF, (iv) Fmoc-Tyr(PO_3H_2)-OH, HBTU, NMM, DMF; (v) piperidine 20%/DMF, (vi) succinic anhydride, NMM, DMF, (vii) 4,7,10-trioxa-1,13-tridecanediamine, HBTU, NMM, DMF; (c) TFA/DCM; (d) 8-azidoATP, CDI-CMD, water, 5 h, rt.

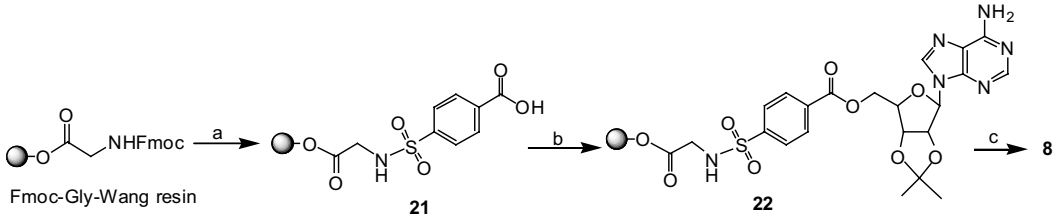

Scheme 3. Synthesis of 4-(carboxymethyl-sulfamoyl)-benzoyladenosine (**8**). Reagents and conditions: (a) (i) piperidine/DMF (1:4), (ii) 4-(chlorosulfonyl)benzoic acid, pyridine/DMF; (b) 2′,3′-*O*-isopropylideneadenosine, DCC, DMAP, DMF/DCM; (c) TFA/DCM.

(**10**) was synthesized using Fmoc-Ile-Wang resin. Reaction of the resin **10** with succinic anhydride in the presence of HBTU and DIEA gave **23** that was reacted with 4,7,10-trioxa-1,13-tridecanediamine under similar conditions to afford **24**. The reaction of 4-(chlorosulfonyl)benzoic acid with the resin **24** in the presence of pyridine afforded **25**. The reaction of the resin **25** with 2′,3′-*O*-isopropylideneadenosine in the presence of DCC and DMAP and the cleavage using TFA afforded **9**.

2.2. Structure–activity relationships

Ac-PYEEI and adenosine derivative **8**, and control pYEEI conjugate with SBA scaffold (**9**) were evaluated against Src tyrosine kinase. Ac-pYEEI had a K_i value of 141.4 μM for polyE$_4$Y phosphorylation that is almost 2-fold higher than K_m for ATP (74 μM) at similar conditions suggesting that this tetrapeptide enhances the catalytic activity. Adenosine derivative (**8**) and SBA-pYEEI conjugate (**9**) did not exhibit any binding affinity to ATP-binding site at maximum tested concentration ($IC_{50} > 300$ μM), thereby they represent compounds with no binding affinity for ATP-binding site. It was found that the SBA-pYEEI conjugate **9** enhanced the catalytic activity and phosphorylation by at least 40%, possibly by activating enzyme through releasing pTyr527 binding with the Src SH2 domain. These results are in agreement with earlier reports[68] indicating that some of the Src SH2 domain inhibitors enhance the catalytic activity.

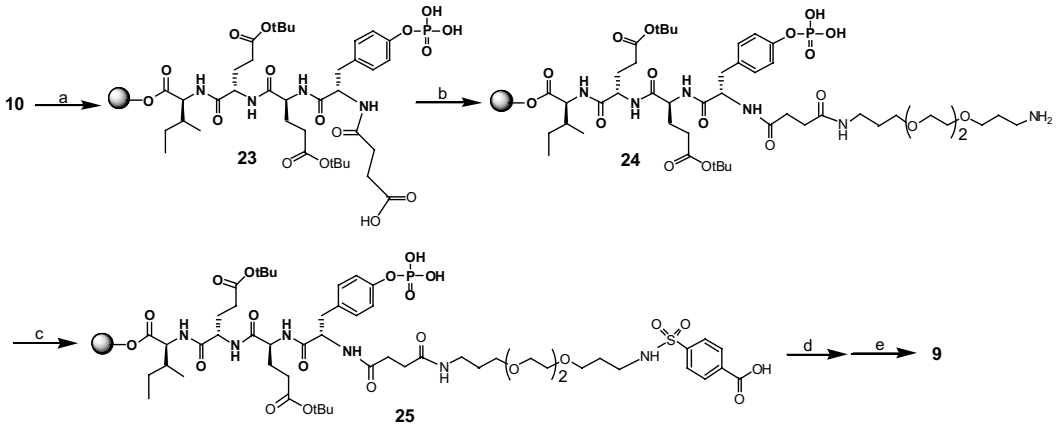

Scheme 4. Synthesis of SBA-Linker-pYEEI derivative **9**. Reagents and conditions: (a) succinic anhydride, DIEA, HBTU, DMF; (b) 4,7,10-trioxa-1,13-tridecanediamine, DIEA, HBTU, DMF; (c) *p*-chlorosulfonylbenzoyl acid, DMF, pyridine; (d) (i) DCC, DMAP, DMF/DCM (ii) 2′,3′-O-isopropylideneadenosine, DMF; (e) TFA/DCM, EDT, H_2O.

Table 1 represents the binding affinity for the synthesized ATP-phosphopeptide conjugates (**1**–**7**) against the Src SH2 domain, Src, and Lck. Steady-state kinetic assays were used to determine the mechanism of interaction of candidate analogs with the ATP-binding site.

In general synthesized ATP-phosphopeptide conjugates may affect Src activity by a variety of mechanisms (**A**–**E**) (Fig. 4) including bivalent binding (**A**), binding to multiple binding sites (**B** and **C**), binding of two ATP-phosphopeptide conjugates (each in one binding site) (**D**), and/or dimer formation (**E**).

The inhibition of wild type Src was compared for the two portions of the ATP-phosphopeptide conjugate: ATP analog and pYEEI. If an inhibitor has any bivalent property, it should display more potent inhibition than either portion alone, or the two components combined in a mixture.

The binding affinities of ATP-phosphopeptide conjugates to the SH2 domain alone versus binding to the SH2 domain in full length Src (KD-Src) for both ATP-phosphopeptide conjugates (**1**–**7**) and AcpYEEI were determined using a fluorescence polarization binding assay according to the methods previously described.[65,66,77] IC_{50} values were assigned to individual compounds according to their competitive binding affinity versus a high-affinity fluorescent peptide probe, fluorescein-Gly-pTyr-Glu-Glu-Ile-NH_2. A reduced IC_{50} value of compounds for the SH2 domain of the full length Src (KD-Src) compared to that for the SH2 domain could suggest that the ATP-phosphopeptide conjugate has a tighter binding to the SH2 domain due to the cooperative binding to another site such as ATP-binding site and/or proper orientation for the binding to the SH2 domain. For compounds with optimal linker size that can accommodate both binding sites in the active form of Src, it was expected that the binding affinities of these analogs to the Src SH2 domain increases when using the whole Src. For ATP-phosphopeptide conjugates without optimal linker size, it was expected than the binding affinity to the whole Src SH2 domain was similar or lower than the SH2 domain alone. The binding affinities of the ATP-phosphopeptide conjugates against the Src SH2 domain (IC_{50} = 11.6–18.5 μM) in a competitive-based assay suggest that these ATP conjugates bind to the Src SH2 domain in a competitive manner. ATP-phosphopeptide conjugate **5** had an approximately 30% better binding affinity to the Src SH2 domain of

Table 1. Screening assays of ATP-phosphopeptide conjugates (**1**–**7**) for binding affinity to the Src SH2 domain and ATP-binding site of Src and Lck

Compound	Src SH2 Domain (IC_{50}, μM)[a]	KD-Src (IC_{50}, μM)[b]	W-Src(K_i, μM)[c]	Lck(K_i, μM)[c]
1	12.4	11.0	10.1	107.8
2	11.6	17.7	11.5	45.5
3	14.3	13.7	14.1	35.5
4	15.1	14.8	15.8	47.2
5	18.5	13.1	1.7	25.3
6	14.5	ND[d]	16.1	42.6
7	35.6	ND[d]	2.6	30.0
AcpYEEI	6.5	7.5	141.4	ND[d]
ATP-γS			57.1	
pYEEI + ATP-γS			7.5	

[a] Binding affinity to the Src SH2 domain using only the Src SH2 domain.
[b] Binding affinity to the Src SH2 domain using whole Src.
[c] Binding affinity to the ATP-binding site.
[d] ND = Not determined.

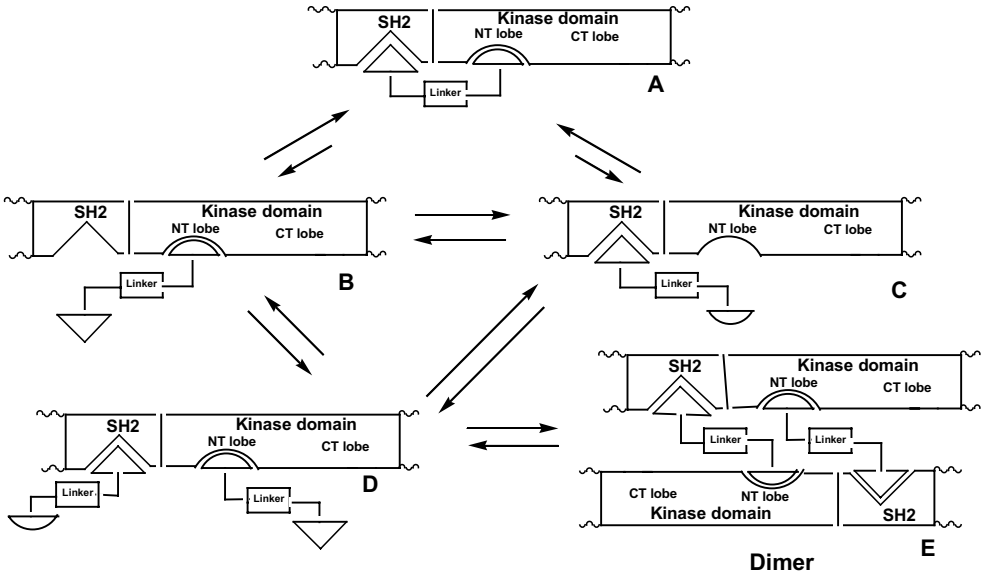

Figure 4. Possible mechanisms for the activity of ATP-phosphopeptide conjugates.

whole Src (KD-Src) (IC_{50} = 13.1 μM) compared to the Src SH2 domain alone (IC_{50} = 18.5 μM), but generally the difference was not significant probably due to the fact that the K_m for binding of ATP portion of the ATP-phosphopeptide is about 74 μM that is 5.6-fold higher than the binding affinity of phosphopeptide AcpYEEI for the SH2 domain (IC_{50} = 6.5 μM). Thus ATP-binding site occupation probably occurs after binding of phosphopeptide portion of ATP-phosphopeptide conjugate to the SH2 domain and cannot contribute to tighter binding of the SH2-directed moiety. In other words, only a fraction of ATP-binding site is probably occupied for cooperative binding of pYEEI to the SH2 domain and for all ATP-phosphopeptide conjugates the mechanism **C** is the most likely starting point and the mechanism **B** does not contribute significantly in the inhibition pattern (Fig. 4). This is based on the fact that pYEEI has higher binding affinity for binding to the SH2 domain than ATP for binding to the ATP-binding site. Designing conjugates with ATP mimics that have higher binding affinity to ATP-binding site than ATP itself may improve the cooperative binding of ATP-phosphopeptide to both binding sites.

On the other hand, one could expect that the binding of pYEEI portion of ATP-phosphopeptide conjugate to the SH2 domain (mechanism **C**) enhances the binding affinity of ATP portion of the ATP-phosphopeptide conjugate to the ATP-binding site if the linker size is optimal for the proper orientation of the ATP inside the binding pocket. The inhibition of substrate phosphorylation by full length active Src and Lck was compared for ATP-phosphopeptide conjugates (**1**–**7**) using a radioactive assay and their K_i values were determined. Most ATP phosphopeptide conjugates (**1**–**4**,**6**) had K_i values of 10.1–16.1 μM. A mixture of AcpYEEI (K_i = 141.4 μM) and ATPγS (K_i = 57.1 μM) in equimolar concentrations inhibited $polyE_4Y$ phosphorylation (K_i = 7.5 μM) that is slightly lower than K_i values of these ATP-phosphopeptide conjugates (**1**–**4**,**6**). Therefore, it is assumed that these ATP-phosphopeptide conjugates do not have optimal linkers for accommodating both binding sites in the active form of Src and the binding to two binding sites is not cooperative. One could expect since the binding affinity for these conjugates to the Src SH2 domain is higher than the ATP-binding site, a larger population of these inhibitors will occupy the Src SH2 domain (mechanism **C**) than the ATP-binding site (mechanism **B**). On the other hand it is possible that two molecules of phosphopeptide-ATP conjugates bind independently from each other to two binding sites in a monovalent pattern (mechanism **D**) resulting in reducing the catalytic activity.

On the other hand, two ATP-phosphopeptide conjugates, **5** and **7**, exhibited tighter inhibition for ATP-binding site of Src (K_i = 1.7–2.6). The mechanism of inhibition against ATP by ATP-phosphopeptide conjugate, **5**, was determined by steady-state kinetics using a radioactive assay in presence of [γ-^{32}P]ATP and different concentrations of ATP. Detailed kinetic studies showed that **5** (K_i = 1.7 μM, V_m = 4.1 pmol/min/U) is a competitive inhibitor against ATP [($K_{m,Src}$(ATP) = 74 μM)] (Fig. 5) as shown a linear competitive pattern of inhibition versus the substrate ATP in double reciprocal plot suggesting that this ATP analog binds to ATP-binding site. ATP-phosphopeptide conjugate **5** was approximately 44-fold more potent than ATP alone suggesting that the binding of pYEEI scaffold of the molecule to the SH2 domain enhances the binding of the ATP-portion of ATP-phosphopeptide conjugate to the ATP-binding site. Since compound **5** binds tighter to ATP-binding site and the Src SH2 domain, the possibility of bivalent binding (mechanism **A**) appears the most likely scenario for this ATP-phosphopeptide analog. Crystallographic structural studies are required to confirm this notion. Similar results were observed for compound **7** having a similar linker length. In case of Lck,

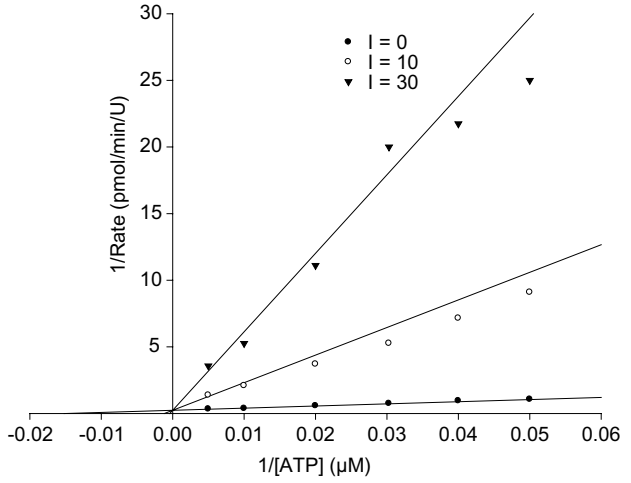

Figure 5. Pattern of inhibition of Src by compound **5**; Lineweaver–Burk plot of $1/V$ versus 1/ATP with varying concentration of **5** shows linear competitive inhibition ($K_i = 1.7\,\mu M$).

conjugates with shorter chain length such as **1** ($K_{i,LcK} = 107.8\,\mu M$) behaved like ATP ($K_{m,LcK} = 98\,\mu M$). Compound **5** ($K_{i,LcK} = 25.3\,\mu M$) with optimal chain length has about 3.9-fold better binding affinity than ATP for binding to ATP-binding site of Lck.

These data indicate that the linking of the ATP and phosphopeptide binding modules could be effective for the inhibition of kinase activity. ATP-phosphopeptide conjugates with optimal linker size such as compound **5** bind to their targets more tightly than ATP by competitively inhibiting both ATP and phosphopeptide binding. These data are in agreement with our earlier studies[76] revealing that a specific distance between the two components of a bivalent ligand is required to achieve an optimal inhibition for cooperative binding.

When the control compound **16** (pYEEI-attached linker, Scheme 1) used alone, the catalytic activity inhibition reduced significantly ($K_i = 608\,\mu M$) possibly due to the activation of the enzyme and enhancement of the substrate phosphorylation. Therefore, the incorporation of two substrate moieties targeting the SH2 domain and ATP-binding site in one molecule as seen in the ATP-phosphopeptide conjugate **5** probably contributes to the bivalent inhibition pattern. The distance between two binding sites in the active form of Src is unknown. The conformation of domains and distance between the SH2 domain and ATP-binding site may also change following the binding of bivalent ligands to any two binding pockets in the active form of Src. The tight inhibition and proper orientation of the first module (phosphopeptide) to the SH2 domain in compound **5** probably leads to the orientation and tight binding of the second motif (ATP) to the ATP-binding site resulting in a bivalent inhibition pattern (**A**). The linkers may assume a loop-like or extended conformation, so that the ATP-binding site-directed fragments associate with ATP-binding site in a structurally compatible fashion.

Cross-linking studies were used to determine whether the dimer formation (mechanism **E**) contributes to the activity of phosphopeptide-ATP conjugates with optimal linker size by cross-linking of the SH2 domain of one Lck molecule with the ATP-binding site of another Lck. A diazido ATP-phosphopeptide conjugate (**7**, Fig. 1) was synthesized using 8-azidoATP and a phosphopeptide, in which the azidophenyl group is attached to P + 1 amino acid of phosphopeptide (Scheme 2). Although the azido-conjugate has lower affinity to the Src SH2 domain ($IC_{50} = 35.6\,\mu M$) probably due to the incorporation of *p*-azido-phenylamino moiety at P + 1 position, the conjugate had a comparable activity with ATP-phosphopeptide conjugate **5** for binding to ATP-binding site ($K_{i,Src} = 2.7\,\mu M$, $K_{i,LcK} = 30.0\,\mu M$). This conjugate was incubated with whole Lck, irradiated with UV light and subjected to SDS-PAGE electrophoresis. The binding affinity of the conjugate for ATP-binding site did not change significantly after UV exposure ($K_{i,LcK} = 29.8\,\mu M$). Only Lck band was observed in all cases indicating the absence of any dimerized product. High molecular weight bands (100 kDa and above) were not observed suggesting that the dimer formation (mechanism **E**) did not contribute to inhibition by phosphopeptide-ATP analog **7** that had a similar linker to compound **5**.

In addition to reducing catalytic activity, compound **5** was approximately 15-fold more selective as inhibitor against Src than Lck. It remains to be seen if this selectivity is observed for other PTKs and serine/threonine kinases. ATP-binding site inhibitors are known to contribute significantly to selectivity against these kinases. ATP is the common substrate for all protein kinases and one could expect that since the ATP portion of ATP-phosphopeptide conjugates binds to all ATP-binding site inhibitors, the high selectivity will not be expected unless the ATP scaffold is replaced with other selective ATP-mimics for a specific kinase.

3. Conclusion

Some SH2 domain inhibitors increase the kinase catalytic activity through activating the kinase. A number of ATP-phosphopeptide conjugates were prepared that contain pYEEI as an SH2 recognition sequence conjugated through a linker to an ATP analog for targeting the ATP-binding site to reduce the kinase catalytic activity resulted from SH2 inhibition and to investigate whether ATP-phosphopeptide conjugates exhibit a higher potency in Src kinase inhibition. ATP-phosphopeptide conjugates that did not have optimal linkers showed that the two modules behaved as independent entities. On the other hand, the inhibition studies with two ATP-phosphopeptide conjugates (**5** and **7**) with optimal linkers suggested that the binding of pYEEI scaffold in these molecules to the SH2 domain causes the ATP portion of the conjugate to bind more tightly to ATP-binding site. The crystal structure of active form of Src has not been determined yet. In future X-ray crystallography studies is required to confirm the bivalent inhibition pattern in the active from of Src.

While many of these ATP-phosphopeptide analogs may not have optimal physicochemical properties, they will provide vital mechanistic information for designing compounds with optimal potency in the future. It is possible to design and synthesize compounds containing appropriate linkers, ATP mimics, and phosphopeptide mimics to improve bioavailability and introduce selectivity for a specific kinase. Conformational rigidity in the linkers can be introduced for the design of bivalent ligands to avoid the compounds become too floppy in binding to the ATP binding pocket and SH2 domain and to avoid unfavorable entropy loss upon binding.

4. Experimental

4.1. General procedure for the synthesis and purification of peptides

In general, all peptides were synthesized by the solid-phase peptide synthesis strategy on a PS3 automated peptide synthesizer (Rainin Instrument Co., Inc.) employing *N*-(9-fluorenyl)methoxycarbonyl (Fmoc) based chemistry on 0.1 mmol of Fmoc-Ile-Wang resin (179 mg, loading capacity 0.56 mmol/g) using Fmoc-amino acid building blocks (0.4 mmol). 2-(1H-Benzotriazole-1-yl)-1,1,3,3-tetramethyluronium hexafluorophosphate (HBTU)/1-hydroxybenzotriazole (HOBt) (0.4 mmol), and NMM (0.4 M) in *N*,*N*-dimethylformamide (DMF) were used as coupling and activating reagents, respectively. Fmoc-Ile-Wang resin, coupling reagents, and Fmoc-amino acid building blocks, including Fmoc-Tyr(PO_3H_2)-OH, Fmoc-Glu(tBu)-OH, Fmoc-Glu-OAll, Fmoc-Glu(PhiPr)-OH, and other Fmoc-aliphatic amino acids were purchased from Novabiochem. Other chemicals and reagents were purchased from Sigma-Aldrich Chemical Company (Milwaukee, WI, USA). Fmoc deprotection at each step was carried out using piperidine in DMF (20%). A mixture of TFA/anisole/water (95:2.5:2.5) was used for side chain deprotection of amino acids and cleavage of the synthesized peptides from the resin. Crude peptides were precipitated by addition of cold diethyl ether (Et_2O) and purified by HPLC (Shimadzu LC-8A preparative liquid chromatograph; Shimadzu fraction collector 10A) on a Phenomenex® Prodigy 10 μm ODS reversed-phase column. Peptides were separated by eluting the crude peptide at 4.0 mL/min using a gradient of 0–100% acetonitrile (0.1% TFA) and water (0.1% TFA) over 85 min and were lyophilized. The purity of final products (>95%) was confirmed by analytical HPLC on a Shimadzu 3 μm C-18 column at 0.5 mL/min using the same gradient system. The chemical structures of compounds were confirmed by a high-resolution PE Biosystems Mariner API time of flight mass spectrometer. Details of procedures and spectroscopic data of representative compounds are presented below.

4.1.1. Synthesis of fluorescent probe fluorescein-Gly-pTyr-Glu-Glu-Ile-NH_2. The fluorescent probe was synthesized, purified, and characterized by coupling of 5-carboxyfluorescein succinimidyl ester with a pentapeptide (Gly-pTyr-Glu-Glu-Ile) as described previously.[65,66,77]

4.1.2. Synthesis of peptides 12–15. Peptides were assembled on Fmoc-Ile-Wang resin using automated solid-peptide synthesis (PS3 peptide synthesizer) via the Fmoc strategy using the general synthetic method described above. Cleavage from the resin and purification of the peptide was carried out as described above in the general procedure to yield **12**–**15** (yields 18–20%). The structures of the peptides were confirmed by electrospray mass spectrometry. Compound **12**: H_2N-βAla-pTyr-Glu-Glu-Ile-OH: $[M]^+$, calcd 704.2; found: 705.3 $[M+H]^+$. Compound **13**: H_2N-6-Ahex-pTyr-Glu-Glu-Ile-OH (6-Ahex = 6-aminohexanoic acid): $[M]^+$, calcd 745.3; found: 746.2 $[M+H]^+$. Compound **14**: H_2N-8-Aoct-pTyr-Glu-Glu-Ile-OH (8-Aoct = 8-aminooctanoic acid): $[M]^+$, calcd 773.3; found: 774.3 $[M+H]^+$. Compound **15**: H_2N-11-Aund-pTyr-Glu-Glu-Ile-OH (11-Aund = 11-aminoundecanoic acid): $[M]^+$, calcd 815.4; found: 816.3 $[M+H]^+$.

4.1.3. Synthesis of peptide H_2N-1,13-Trioxa-Suc-pTyr-Glu-Glu-Ile-OH (1,13-Trioxa = 4,7,10-trioxa-1,13-tridecanediamine; Suc = succinoyl) (16). The peptide sequence pTyr-Glu-Glu-Ile was assembled on Wang resin (using 0.1 mmol Fmoc-Ile-Wang resin). The Fmoc group on the N-terminal of the p-Tyr moiety was removed using piperidine in DMF (20%, 5 mL × 2). The resin was washed with acetic acid in DMF (1%, 50 mL), TEA in DMF (1%, 50 mL), and DMF (50 mL), followed by MeOH (50 mL) and DCM (50 mL), respectively. The obtained resin was completely dried under vacuum, then suspended in dry DMF (5 mL), to which an excess of succinic anhydride (300 mg, 3 mmol) was added. The suspension was mixed for 2 h at room temperature. The solvent was removed by filtration and the resin was washed with TEA in DMF (1%, 50 mL), DMF (50 mL), MeOH (50 mL), and DCM (50 mL), respectively. The resin was then dried under vacuum overnight and suspended in dry DMF (5 mL). To the swelled resin, HBTU (150 mg, 0.4 mmol) was added, followed by 4,7,10-trioxa-1,13-tridecanediamine (176 μL, 0.8 mmol). The resulting suspension was mixed at room temperature for 3 h, then the solvent was filtered off. The resin was washed with DMF (50 mL), MeOH (50 mL), DCM (50 mL), respectively, and dried under vacuum for 30 min. Cleavage of the peptide from the resin and subsequent purification were carried out as described in the general procedure to yield **16** (20%). The identity of the peptide was confirmed by electrospray mass spectrometry. $[M]^+$, calcd 934.4; found: 935.3 $[M+H]^+$.

4.1.4. Synthesis of peptide (H_2N-1,8-Diam-Suc-1,8-Diam-Suc-pTyr-Glu-Glu-Ile-OH (1,8-Diam = 1,8-diamino-3,6-dioxaoctane; Suc = succinoyl) (17). The peptide sequence pTyr-Glu-Glu-Ile was assembled on Wang resin (using 0.1 mmol Fmoc-Ile-Wang resin). The Fmoc group on the N-terminal of the pTyr moiety was removed using piperidine in DMF (20%, 5 mL × 2). The resin was washed with acetic acid in DMF (1%, 50 mL), TEA in DMF (1%, 50 mL), and DMF (50 mL), MeOH (50 mL), and DCM (50 mL),

respectively. The obtained resin was completely dried under vacuum, then suspended in dry DMF (5 mL), to which an excess of succinic anhydride (300 mg, 3 mmol) was added. The suspension was mixed for 2 h at room temperature. The solvent was removed by filtration and the resin was washed with TEA in DMF (1%, 50 mL), and DMF (50 mL), MeOH (50 mL), and DCM (50 mL), respectively. The resin was dried under vacuum overnight and suspended in dry DMF (5 mL). To the swelled resin in DMF was added HBTU (150 mg, 0.4 mmol), followed by 1,8-diamino-3,6-dioxaoctane (100 μL, 0.8 mmol). The resulting suspension was mixed at room temperature for 3 h, then the solvent was filtered off. The resin was washed with DMF (50 mL), MeOH (50 mL), DCM (50 mL), respectively, and dried under vacuum overnight. Coupling of succinic anhydride and 1,8-diamino-3,6-dioxaoctane was repeated again for one more cycle as described above. Cleavage of the peptide from the resin and subsequent purification were carried out as described above in the general procedure to yield **17** (18%). The identity of the peptide was confirmed by electrospray mass spectrometry. $[M]^+$, calcd 1092.5; found: 1093.4 $[M+H]^+$.

4.1.5. Synthesis of 1,13-Trioxa-SA-pTyr-g-*p*-azidoGlu-Glu-Ile-OH (20). The resin-bound peptide **18** (0.1 mmol) was synthesized on Wang resin using an automated peptide synthesizer (PS3) via Fmoc peptide strategy. The resin **18** was suspended in TFA/DCM/TIPS (5:90:5, 5 mL) and the resulting suspension was mixed for 1 h to remove the Ph*i*Pr (2-phenylisopropyl) protecting group on the γ-carboxylic moiety of the β-glutamic acid. The deprotection was repeated with one more cycle. The resin was washed with DMF (50 mL), MeOH (50 mL), and DCM (50 mL), respectively, and was completely dried under vacuum overnight. The dry resin was suspended in dry DMF (5 mL). To the resulting suspension was added HBTU (153 mg, 0.4 mmol), *p*-azidoaniline (56 mg, 0.4 mmol), and NMM (100 μL). The reaction mixture was covered with aluminum foil and mixed for 3 h at room temperature. The solvent was filtered off and the resin was washed with DMF (50 mL), MeOH (50 mL), and DCM (50 mL), respectively. The resin was then suspended in piperidine/DMF (20%, 5 mL) and mixed for 5 min to unmask the amino group of the N-terminal. This step was repeated once. The resin was then washed with DMF (50 mL), MeOH (50 mL), and DCM (50 mL), respectively, and dried under vacuum overnight. The unmasked amino group was reacted with excess succinic anhydride (200 mg, 2 mmol) to a suspension of the resin in dry DMF (5 mL) for 3 h at room temperature. The solvent was filtered off and the resin was washed with DMF (50 mL), MeOH (50 mL), and DCM (50 mL), respectively, and dried completely under vacuum. The dry resin was suspended again in dry DMF (5 mL), to which HBTU (153 mg, 0.4 mmol), 4,7,10-trioxa-1,13-tridecanediamine (88 μL, 0.4 mmol), and NMM (100 μL) were added. The mixture was mixed for 3 h at room temperature. After that, the resin was washed with DMF (50 mL), MeOH (50 mL), and DCM (50 mL), and dried under vacuum for 30 min to give the resin-bound peptide **19**. Cleavage of **19** using TFA as described in the general section afforded peptide **20** (47 mg, 45%). MS (ESI) $[M]^+$, calcd 1051.4; found: 1052.4 $[M+H]^+$.

4.2. Synthesis of ATP-phosphopeptide conjugates

4.2.1. Synthesis of ATP-βAla-pTyr-Glu-Glu-Ile-OH (1). Adenosine 5′-triphosphate disodium salt (30 mg, 54.3 μmol) was dissolved in distilled water (5 mL) and the pH of the solution was brought to 7 (using pH paper indicator) by titrating with sodium hydroxide (1 M). *N*-Cyclohexyl-*N*′-(2-morpholinoethyl)carbodiimide methyl-*p*-toluene sulfonate (382 mg, 0.90 mmol) and additional water (1 mL) were added to the reaction mixture. The pH of solution was brought down to 5.6 with HCl (1 M) and maintained in a pH range between 5.6 and 5.8 throughout the reaction as determined by pH paper. Peptide **12** (15 mg, 21.6 μmol) dissolved in DMF (1 mL) was added to the solution and the reaction mixture was titrated back to pH 5.6–5.8 with sodium hydroxide (1 M). The reaction was left stirring for an additional 4 h and then treated with triethylamine to reach pH 8.5. The mixture was purified on a DEAE Sephadex-A25 anion exchange column with pH 8 triethylammonium bicarbonate (TEAB) buffer. Briefly, a Sephadex DEAE A25 (6 g) was swelled in water, placed into a column, washed with water (100 mL), TEAB (1 M, 100 mL) and again water (175 mL). A gradient system was used for purifications (A = water, B = TEAB 1 M) using a flow rate of 3 mL/min and fraction sizes of 6 mL at 4 °C; gradient: 0–60 mL, B (0%); 60–260 mL, B (0–40%), 260–360 mL, B (40–100%). Compound **1** was eluted in 60% TEAB (9.2 mg, 35.7%). MS (ESI) $[M]^+$, calcd 1192.2; found: 1193.3 $[M+H]^+$, 1214.2 $[M+Na]^+$, 1292.2 $[M+TEA]^+$, 1392.2 $[M+2TEA]^+$.

4.2.2. Synthesis of ATP-6-Ahex-pTyr-Glu-Glu-Ile-OH (2). A similar strategy as described above for the preparation and purification of ATP-phosphopeptide conjugate **1** was followed using adenosine 5′-triphosphate disodium salt (35 mg, 63.7 μmol), *N*-cyclohexyl-*N*′-(2-morpholinoethyl)carbodiimide methyl-*p*-toluene sulfonate (382 mg, 0.90 mmol) and peptide **13** (20 mg, 26.9 μmol). Compound **2** was eluted in 60% TEAB (7.3 mg, 21.9%). MS (ESI) $[M]^+$, calcd 1234.2; found: 1235.3 $[M+H]^+$, 1256.2 $[M+Na]^+$, 1334.5 $[M+TEA]^+$, 1434.4 $[M+2TEA]^+$.

4.2.3. Synthesis of ATP-8-Aoct-pTyr-Glu-Glu-Ile-OH (3). A similar strategy as described above for the preparation of ATP-phosphopeptide conjugate **1** was followed using adenosine 5′-triphosphate disodium salt (35 mg, 63.7 μmol), *N*-cyclohexyl-*N*′-(2-morpholinoethyl)carbodiimide methyl-*p*-toluene sulfonate (382 mg, 0.90 mmol) and peptide **14** (23 mg, 29.7 μmol). Compound **3** was eluted in 60% TEAB (6.5 mg, 17.3%). MS (ESI) $[M]^+$, calcd 1262.3; found: 1263.3 $[M+H]^+$, 1306.3 $[M+Na]^+$, 1334.5 $[M+TEA]^+$, 1372.3 $[M+5Na]^+$, 1450.4 $[M+4Na+TEA]^+$.

4.2.4. Synthesis of ATP-11-Aund-pTyr-Glu-Glu-Ile-OH (4). A similar strategy as described above for the preparation of ATP-phosphopeptide conjugate **1** was followed using adenosine 5′-triphosphate disodium salt

(35 mg, 63.7 μmol), *N*-cyclohexyl-*N*′-(2-morpholinoethyl)carbodiimide methyl-*p*-toluene sulfonate (382 mg, 0.90 mmol) and peptide **15** (21 mg, 25.7 μmol). Compound **4** was eluted in 65% TEAB (7.1 mg, 21.2%). MS (ESI) $[M]^+$, calcd 1304.5; found: 1305.5 $[M+H]^+$, 1326.3 $[M+Na]^+$, 1404.5 $[M+TEA]^+$, 1504.4 $[M+2TEA]^+$.

4.2.5. Synthesis of ATP-1,13-Trioxa-Suc-pTyr-Glu-Glu-Ile-OH (5). A similar strategy as described above for the preparation of ATP-phosphopeptide conjugate **1** was followed using adenosine 5′-triphosphate disodium salt (40 mg, 72.8 μmol), *N*-cyclohexyl-*N*′-(2-morpholinoethyl)carbodiimide methyl-*p*-toluene sulfonate (382 mg, 0.90 mmol) and peptide **16** (25 mg, 26.7 μmol). Compound **5** was eluted in 65–70% TEAB (5.7 mg, 14.9%). MS (ESI) $[M]^+$, calcd 1423.4; found: 1424.4 $[M+H]^+$, 1445.4 $[M+Na]^+$, 1523.4 $[M+TEA]^+$, 1623.4 $[M+2TEA]^+$.

4.2.6. Synthesis of ATP-1,8-Diam-Suc-1,8-Diam-Suc-p-Tyr-Glu-Glu-Ile-OH (6). A similar strategy as described above for the preparation of ATP-phosphopeptide conjugate **1** was followed using adenosine 5′-triphosphate disodium salt (50 mg, 91.1 μmol), *N*-cyclohexyl-*N*′-(2-morpholinoethyl)carbodiimide methyl-*p*-toluene sulfonate (382 mg, 0.90 mmol) and peptide **17** (21 mg, 19.2 μmol). Compound **6** was eluted in 65–70% TEAB (5.2 mg, 16.9%). MS (ESI) $[M]^+$, calcd 1598.5; found: 1599.4 $[M+H]^+$, 1620.5 $[M+Na]^+$, 1698.5 $[M+TEA]^+$.

4.2.7. Synthesis of ATP-1,13-Trioxa-SA-pTyr-g-*p*-azido-Glu-Glu-Ile-OH (7). 8-Azidoadenosine 5′-triphosphate disodium salt (25 mg, 45.5 μmol) was dissolved in distilled water (5 mL) and the pH of the solution was brought to 7 (using pH paper indicator) by titrating with sodium hydroxide (1 M). *N*-Cyclohexyl-*N*′-(2-morpholinoethyl)carbodiimide methyl-*p*-toluene sulfonate (382 mg, 0.90 mmol) was added to the reaction mixture with another 1 mL water. The pH of solution was brought down to 5.6 with HCl (1 M) and maintained in a pH range between 5.6 and 5.8 throughout the reaction as determined by pH paper. Peptide **20** (29 mg, 27.5 μmol) in DMF (1 mL) was added to the solution and the reaction mixture was titrated back to pH 5.6–5.8 with sodium hydroxide (1 M). The reaction was covered with aluminum foil and left stirring for an additional 4 h and then treated with triethylamine to reach pH 8.5. The mixture was purified on a DEAE Sephadex-A25 anion exchange column (covered with aluminum foil) with pH 8 triethylammonium bicarbonate (TEAB) buffer as described above for ATP-phosphopeptide conjugate **1**. Compound **7** was eluted in 55–60% TEAB (13.9 mg, 32.0%). MS (ESI) $[M]^+$, calcd 1580.4; found: 1581.4 $[M+H]^+$, 1602.5 $[M+Na]^+$, 1680.5 $[M+TEA]^+$.

4.3. Synthesis of sulfamoyl adenosine derivatives (8,9)

4.3.1. Synthesis of 4-(carboxymethylsulfamoyl)benzoyl-adenosine (8). The Fmoc-Gly-Wang resin (175 mg, 0.56 mmol/g) was swelled in dry DMF (5 mL, 10 min). After the solvent was drained, the resin was suspended in piperidine in DMF (20%, 5 mL, 5 min) to remove the Fmoc group. Fmoc deprotection was repeated once. The resin was washed with DMF (50 mL), MeOH (50 mL), and DCM (50 mL), respectively, and dried under vacuum. Pyridine (0.5 mL) and 4-(chlorosulfonyl)benzoic acid (110 mg, 0.5 mmol) were added in portions over 30 min to the swelled resin in dry DMF (5 mL). The mixture was shaken for 24 h at room temperature. The solvents were then filtered off and the resin was washed with TEA in DMF (1%, 50 mL), DMF (50 mL), MeOH (50 mL) and DCM (50 mL), respectively, to yield **21**. The resin **21** was dried under vacuum overnight, then swelled in dry DMF (3 mL) and dry DCM (3 mL). The resulting suspension was cooled to 0 °C using an ice bath and DCC (103 mg, 0.5 mmol) was added in one portion, followed by DMAP (12 mg, 0.1 mmol). After 25 min, a solution of 2′,3′-*O*-isopropylideneadenosine (153 mg, 0.5 mmol) in dry DMF(1 mL) was added. The suspension was mixed for 6 h at room temperature. The resin was filtered off and dried under vacuum for 30 min to yield **22**. Cleavage of 4-(carboxymethylsulfamoyl)benzoyladenosine (**8**) from the resin **22** was carried out using TFA as described in general section (21 mg, 42%). The identity of the compound was confirmed by ^{1}H NMR and electrospray mass spectrometry. ^{1}H NMR ($CDCl_3$, 400 MHz) δ 7.41–7.72 (m, 6H), 5.55 (d, $J = 3$ Hz, 1 H), 4.05–4.45 (m, 7H). MS (ESI) $[M]^+$, calcd 508.1; found: 509.3 $[M+H]^+$.

4.3.2. Synthesis of SBA-linker-pYEEI derivatives (9). The resin-bound pYEEI peptide **10** was synthesized using Fmoc-Ile-Wang resin (175 mg, 0.56 mmol/g) as described above. The resin was completely dried and suspended in dry DMF (5 mL, 10 min). Succinic anhydride (80 mg, 0.8 mmol), HBTU (300 mg, 0.8 mmol), and DIEA (0.5 mL) were added. The content was mixed for 3 h at room temperature. After that, the solvents were drained and the resin was washed with DMF (50 mL), MeOH (50 mL), and DCM (50 mL), respectively, to yield **23**. The resin **23** was completely dried and suspended in dry DMF (5 mL, 10 min), to which 4,7,10-trioxa-1,13-tridecanediamine (100 mg, 0.5 mmol), HBTU (170 mg, 0.5 mmol), and DIEA (0.3 mL) were added. The content was mixed for 3 h at room temperature. After that, the solvents were drained and the resin was washed with DMF (50 mL), MeOH (50 mL), and DCM (50 mL), respectively, and dried under vacuum to yield **24**. 4-(Chlorosulfonyl)benzoic acid (110 mg, 0.5 mmol) in portions over 30 min was added to the swelled resin **24** in dry DMF (5 mL) and pyridine (0.5 mL). The suspension was mixed for 24 h at room temperature. The solvents were then filtered off and the resin was washed with TEA in DMF (1%, 50 mL), DMF (50 mL), MeOH (50 mL) and DCM (50 mL), respectively, to yield **25**. The resin **25** was dried under vacuum overnight, then suspended in dry DMF (3 mL) and dry DCM (3 mL). The resulting suspension was cooled to 0 °C using an ice bath and DCC (103 mg, 0.5 mmol) was added in one portion, followed by DMAP (12 mg, 0.1 mmol). After 25 min, a solution of 2′,3′-*O*-isopropylideneadenosine (153 mg, 0.5 mmol) in dry DMF (1 mL) was added. The suspension was mixed for 6 h at room temperature. The resin was filtered off

and dried under vacuum for 30 min. The cleavage reaction was carried out using TFA as described in general section to yield **9** (71 mg, 53%). The identity of the compound was confirmed by electrospray mass spectrometry. $[M]^+$, calcd 1367.4; found: 1367.5 $[M]^+$, 1389.4 $[M+Na]^+$.

4.4. Protein expression and purification

The Src SH2 domain and Lck were expressed and purified according to previously reported methods.[65–67,78,79] The Src SH2 domain was purified as fusion with GST. Active Src p60c-Src (14-117) was purchased from Upstate Signaling Solution and was not phosphorylated on the regulatory C-terminal tail and consequently existed in an activated state.

4.5. Src SH2 domain binding assay

The binding to the SH2 domain alone versus binding to full length of these Src kinases for both ATP-phosphopeptide conjugates and parent structures were determined using a fluorescence polarization (FP) binding assay according to previously reported methods.[65,66,77] IC_{50} values were assigned to individual compounds according to their competitive binding affinity versus a high-affinity peptide probe, fluorescein-Gly-pTyr-Glu-Glu-Ile-NH_2. All assays were performed in triplicate. For ATP-phosphopeptide conjugate **7**, the same experimental procedures were followed except that after incubation with the Src SH2 domain for 10 min, the reaction mixture containing the compound was radiated with short-wave UV (254 nm) for 1 h then with long-wave UV (365 nm) for 1 h. The inhibition percentages were calculated and the IC_{50} values were obtained by using Curve-Fitting software (CurveExpert 3.1).

4.6. Steady-state kinetic assays

Steady-state kinetic assays with Src or Lck were carried out using a radioactive assay to evaluate mechanisms of inhibition by ATP-phosphopeptide conjugates relative to natural substrate ATP. Artificial substrate polyE_4Y (average MW: 35 kD) was used for routine kinase activity. The kinase activity of PTKs was first determined using a standard radiometric PTK activity assay. This assay contains polyE_4Y as the phosphate accepting substrate, [γ-^{32}P]-ATP, and $MgCl_2$. After a reaction time of 30 min at 30 °C, 35 μl of the reaction mixture was removed and spotted onto a filter paper and placed into warm 5% trichloroacetic acid (TCA). The TCA stops the kinase reaction, precipitates the proteins and poly-E_4Y onto the filter paper, and washes the unreacted ATP and others away. After three TCA washes for 10 min each, the radioactivity remaining on the filter paper was determined by liquid scintillation counting. The assays were done in duplicates and repeated at least three times. Control reactions lacking polyE_4Y were included for each enzyme concentration to correct for any nonpolyE_4Y specific phosphorylation. Percentage of inhibition was plotted as a function of the compound concentration and the IC_{50} value (the concentration of a compound that caused 50% inhibition) was obtained from such a plot. To determine the inhibitory mechanism with regard to ATP, the K_m and V_m values with ATP as the variable substrate was determined at various concentrations of ATP-phosphopeptide conjugates **5** and **7** while other components of the assay were at fixed concentrations using Lineweaver double reciprocal plots. The inhibitory mechanism was determined based on the effect of the compound on the K_m and V_m values. Inhibitory constant (K_i) was determined by using Sigma Plot 8.0 Enzyme Kinetics Module. For mixed experiments using ATPγS mixture with pYEEI, same molar concentrations were used for each component.

4.7. Cross-linking experiment using diazido conjugate 7

Diazido conjugate **7** (1.2 mg) was dissolved in kinase buffer (265 μL) to make a stock solution of 3000 μM. The reaction mixtures were prepared with the final concentrations of **7** (50 or 500 μM), $MgCl_2$ (12 mM), and Lck (80 μM). The reaction mixtures were allowed to incubate for 10 min at room temperature, placed in a dark chamber, and irradiated with long wave UV 365 nm for 1.5 h or short wave UV 254 nm for 1 h and long wave 365 nm for 1 h. Control reaction mixtures prepared in the absence of UV and/or ATP-phosphopeptide conjugate **7**. All reaction mixtures were denatured by incubation at 95–100 °C for 5 min. A loading buffer containing bromophenol blue (10 μL) was added. The reaction mixtures were subjected to SDS-PAGE by loading into a gel (7%) and running for 2.5 h. The gel was stained using Coomassie Blue (G95) using a standard protocol for protein staining.

Acknowledgements

We acknowledge the financial support from BRIN/INBRE Program of the National Center for Research Resources, NIH, Grant number 1 P20 RR16457 and Rhode Island Foundation, Grant number 20030201.

References and notes

1. Klint, P.; Claesson-Welsh, L. *Front Biosci.* **1999**, *4*, D165.
2. Dominguez, M.; Wasserman, J. D.; Freeman, M. *Curr. Biol.* **1998**, *8*, 1039.
3. Sieg, D. J.; Hauck, C. R.; Ilic, D.; Klingbeil, C. K.; Schaefer, E.; Damsky, C. H.; Schlaepfer, D. D. *Nature Cell Biol.* **2000**, *2*, 249.
4. Casaccia-Bonnefil, P.; Gu, C.; Chao, M. V. *Adv. Exper. Med. Biol.* **1999**, *468*, 275.
5. Druker, B. J. *Semin. Hematol.* **2003**, *40*, 50.
6. Wakeling, A. E. *Curr. Opin. Pharmacol.* **2002**, *2*, 382–387.
7. Slamon, D. J.; Leyland-Jones, B.; Shak, S.; Fuchs, H.; Paton, V.; Bajamonde, A.; Fleming, T.; Eiermann, W.; Wolter, J.; Pegram, M.; Baselga, J.; Norton, L. *N. Engl. J. Med.* **2001**, *344*, 783.
8. Ferrara, N.; Hillan, K. J.; Gerber, H.-P.; Novotony, W. *Nat. Rev. Drug Dis.* **2004**, *3*, 391.

9. Warmuth, M.; Damoiseaux, R.; Liu, Y.; Fabbro, D.; Gray, N. *Curr. Pharm. Des.* **2003**, *9*, 2043.
10. Biscardi, J. S.; Tice, D. A.; Parsons, S. J. *Adv. Cancer Res.* **1999**, *76*, 61.
11. Avizienyte, E.; Wyke, A. W.; Jones, R. J.; McLean, G. W.; Westhoff, M. A.; Brunton, V. G.; Frame, M. C. *Nat. Cell Biol.* **2002**, *4*, 632.
12. Lowell, C. A.; Berton, G. *J. Leukoc. Biol.* **1999**, *65*, 313.
13. Missbach, M.; Jeschke, M.; Feyen, J.; Muller, K.; Glatt, M.; Green, J.; Susa, M. *Bone* **1999**, *24*, 437.
14. Shakespeare, W.; Yang, M.; Bohacek, R.; Cerasoli, F.; Stebbins, K.; Sundaramoorthi, R.; Azimioara, M.; Vu, C.; Pradeepan, S.; Metcalf, C.; Haraldson, C.; Merry, T.; Dalgarno, D.; Narula, S.; Hatada, M.; Lu, X.; van Schravendijk, M. R.; Adams, S.; Violette, S.; Smith, J.; Guan, W.; Bartlett, C.; Herson, J.; Iuliucci, J.; Weigele, M.; Sawyer, T. *Proc. Natl. Acad. Sci. U.S.A.* **2000**, *97*, 9373.
15. Luttrell, D. K.; Lee, A.; Lansing, T. J.; Crosby, R. M.; Jung, K. D.; Willard, D.; Luther, M.; Rodriguez, M.; Berman, J.; Gilmer, T. M. *Proc. Natl. Acad. Sci. U.S.A.* **1994**, *91*, 83.
16. Frame, M. *Biochim. Biophys. Acta* **2002**, *1602*, 114.
17. Weber, T. K.; Steele, G.; Summerhayes, I. C. *J. Clin. Invest.* **1992**, *90*, 815.
18. Ottenholf-Kalff, A. E.; Rijksen, G.; van Beurden, E. A.; Hennipman, A.; Michels, A. A.; Staal, G. E. *Cancer Res.* **1992**, *49*, 4773.
19. Thomas, S. M.; Brugge, J. S. *Annu. Rev. Cell Dev. Biol.* **1997**, *13*, 513.
20. Lowe, C.; Yoneda, T.; Boyce, B. F.; Chen, H.; Mundy, G. R.; Soriano, P. *Proc. Nat. Acad. Sci. U.S.A.* **1993**, *90*, 4485.
21. Boyce, B. F.; Yoneda, T.; Lowe, C.; Soriano, P.; Mundy, G. R. *J. Clin. Invest.* **1992**, *90*, 1622.
22. Soriano, P.; Montgomery, C.; Geske, R.; Bradley, A. *Cell* **1991**, *64*, 693.
23. Xu, W.; Doshi, A.; Lei, M.; Eck, M. J.; Harrison, S. C. *Mol. Cell* **1999**, *3*, 629.
24. Songyang, Z.; Shoelson, S. E.; Chaudhuri, M.; Gish, G.; Pawson, T.; Haser, W. G.; King, F.; Roberts, T.; Ratnofsky, S.; Lechleider, R. J.; Neel, B. G.; Birge, R. B.; Fajardo, J. E.; Chou, M. M.; Hanatusa, H.; Schaffhausen, B.; Cantley, L. C. *Cell* **1993**, *72*, 767.
25. Sadowski, I.; Stone, J. C.; Pawson, T. *Mol. Cell. Biol.* **1986**, *6*, 4396.
26. Cantley, L. C.; Auger, K. R.; Carpenter, C.; Duckworth, B.; Graziana, A.; Kapeller, R.; Soltoff, S. *Cell* **1991**, *64*, 281.
27. Fukui, Y.; Hanafusa, H. *Mol. Cell. Biol.* **1991**, *11*, 1972.
28. Schaller, M. D.; Hilderbrand, J. D.; Shannon, J. D.; Fox, J. W.; Vines, R. R.; Parsons, J. T. *Mol. Cell. Biol.* **1994**, *14*, 1680.
29. Taylor, S. J.; Shalloway, D. *Nature* **1994**, *368*, 867.
30. Petch, L. A.; Bockholt, S. M.; Bouton, A.; Parsons, J. T.; Burridge, K. *J. Cell. Sci.* **1995**, *108*, 1371.
31. Sawyer, T. K. *Biopolymers* **1998**, *47*, 243.
32. Vu, C. B.; Corpuz, E. G.; Pradeepan, S. G.; Violette, S.; Bartlett, C.; Sawyer, T. K. *Bioorg. Med. Chem. Lett.* **1999**, *9*, 3009.
33. Vu, C. B. *Curr. Med. Chem.* **2000**, *7*, 1081.
34. Muller, G. *Topics Curr. Chem.* **2000**, *211*, 17.
35. Vu, C. B.; Corpuz, E. G.; Merry, T. J.; Pradeepan, S. G.; Bartlett, C.; Bohacek, R. S.; Botfield, M. C.; Eyermann, C. J.; Lynch, B. A.; MacNeil, I. A.; Ram, M. K.; van Schravendijk, M. R.; Violette, S.; Sawyer, T. K. *J. Med. Chem.* **1999**, *42*, 4088.
36. Cody, W. L.; Lin, Z.; Panek, R. L.; Rose, D. W.; Rubin, J. R. *Curr. Pharm. Des.* **2000**, *6*, 59.
37. Showalter, H. D.; Kraker, A. J. *Pharmacol. Ther.* **1997**, *76*, 55.
38. Traxler, P. *Expert Opin. Ther. Patents* **2003**, *7*, 215.
39. Levitzki, A. *Acc. Chem. Res.* **2003**, *36*, 462.
40. Rossé, G.; Séquin, U.; Mett, H.; Furet, P.; Traxler, P.; Fretz, H. *Helv. Chim. Acta* **1997**, *80*, 653–670.
41. Yuan, C. J.; Jakes, S.; Elliot, S.; Graves, D. *J. Biol. Chem.* **1990**, *265*, 16205.
42. Cushman, M.; Chinnasamy, P.; Chakraborti, A. K.; Jurayj, J.; Geahlen, R. L.; Haugwitz, R. D. *Int. J. Pept. Protein Res.* **1990**, *36*, 538.
43. Bohmer, F. D.; Kaagyozov, L.; Uecker, A.; Serve, H.; Botzki, A.; Mahboobi, S.; Dove, S. *J. Biol. Chem.* **2003**, *14*, 5148.
44. Huse, M.; Kuriyan, J. *Cell* **2002**, *109*, 275.
45. Topaly, J.; Zeller, W. J.; Fruehauf, S. *Leukemia* **2001**, *15*, 342.
46. Thiesing, J. T.; Ohno-Jones, S.; Kolibaba, K. S.; Druker, B. J. *Blood* **2000**, *96*, 3195.
47. Buchdunger, E.; Cioffi, C. L.; Law, N.; Stiver, D.; Ohno-Jones, S.; Druker, B. J.; Lyndon, N. B. *J. Pharmacol. Exp. Ther.* **2000**, *295*, 139.
48. Okuda, K.; Weisberg, E.; Gilliland, D. G.; Griffin, J. D. *Blood* **2001**, *97*, 2440.
49. Wakeling, A. E.; Guy, S. P.; Woodburn, J. R.; Ashton, S. E.; Curry, B. J.; Barker, A. J.; Gibson, K. H. *Cancer Res.* **2002**, *62*, 5749.
50. Schultz, J. *J. Natl. Cancer. Inst.* **2003**, *95*, 577.
51. Marseigne, I.; Roques, B. P. *J. Org. Chem.* **1988**, *53*, 3621.
52. Burke, T. R., Jr.; Russ, P.; Lim, B. *Synthesis* **1991**, *11*, 1019.
53. Shoelson, S. E.; Chatterjee, S.; Chaudhuri, M.; Burke, T. R., Jr. *Tetrahedron Lett.* **1991**, *32*, 6061.
54. Smyth, M. S.; Ford, H.; Burke, T. R., Jr. *Tetrahedron Lett.* **1992**, *33*, 4137.
55. Burke, T. R., Jr.; Smyth, M. S.; Nomizu, M.; Otaka, A.; Roller, P. R. *J. Org. Chem.* **1993**, *58*, 1336.
56. Burke, T. R., Jr.; Smyth, M. S.; Otaka, A.; Nomizu, M.; Roller, P. P.; Wolf, G.; Case, R.; Shoelson, S. E. *Biochemistry* **1994**, *33*, 6490.
57. Yao, Z. J.; King, C. R.; Cao, T.; Kelley, J.; Milne, G. W. A.; Voigt, J. H.; Burke, T. R. *J. Med. Chem.* **1999**, *42*, 25.
58. Shahripour, A.; Plummer, M. S.; Lunney, E. A.; Para, K. S.; Stankovic, C. J.; Rubin, J. R.; Humblet, C.; Fergus, J. H.; Marks, J. S.; Herrera, R.; Hubbell, S. E.; Saltiel, A. R.; Sawyer, T. K. *Bioorg. Med. Chem. Lett.* **1996**, *6*, 1209.
59. Sundaramoorthi, R.; Kawahata, N.; Yang, M. G.; Shakespeare, W. C.; Metcalf, C. A., III; Wang, Y.; Merry, T.; Eyermann, C. J.; Bohacek, R. S.; Narula, S.; Dalgarno, D. C.; Sawyer, T. K. *Biopolymers* **2003**, *71*, 717.
60. Ye, B.; Akamatsu, M.; Shoelson, S. E.; Wolf, G.; Giorgetti-Peraldi, S.; Yan, X.; Roller, P. P.; Burke, T. R., Jr. *J. Med. Chem.* **1995**, *38*, 4270.
61. Burke, T. R.; Yao, Z. J.; Zhao, H.; Milne, G. W. A.; Wu, L.; Zhang, Z. Y.; Voigt, J. H. *Tetrahedron* **1998**, *54*, 9981.
62. Gao, Y.; Burke, T. R. *Synlett* **2000**, *1*, 134.
63. Gao, Y.; Luo, J.; Yao, Z. J.; Guo, R. B.; Zou, H.; Kelley, J.; Voigt, J. H.; Yang, D. J.; Burke, T. R. *J. Med. Chem.* **2000**, *43*, 911.
64. Tong, L.; Warren, T. C.; Lukas, S.; Schembri-King, J.; Betageri, R.; Proudfoot, J. R.; Jakes, S. *J. Biol. Chem.* **1998**, *273*, 20238.
65. Nam, N. H.; Pitts, R.; Sun, G.; Sardari, S.; Tiemo, A.; Xie, M.; Yan, B.; Parang, K. *Bioorg. Med. Chem.* **2004**, *12*, 779.

66. Nam, N. H.; Ye, G.; Sun, G.; Parang, K. *J. Med. Chem.* **2004**, *47*, 3131.
67. Sicheri, F.; Moarefi, I.; Kuriyan, J. *Nature* **1997**, *385*, 602.
68. Mandine, E.; Jean-Baptiste, V.; Vayssiere, B.; Gofflo, D.; Benard, D.; Sarubbi, E.; Deprez, P.; Baron, R.; Superti-Furga, G.; Lesuisse, D. *Biochem. Biophys. Res. Commun.* **2002**, *298*, 185.
69. Liu, X.; Brodeur, S. R.; Gish, G.; Songyang, Z.; Cantley, L. C.; Laudano, A. P.; Pawson, T. *Oncogene* **1993**, *8*, 1119.
70. Alonso, G.; Koegl, M.; Mazurenko, N.; Courtneidge, S. A. *J. Biol. Chem.* **1995**, *270*, 9840.
71. Boerner, R. J.; Kassel, D. B.; Barker, S. C.; Ellis, B.; DeLacy, P.; Knight, W. B. *Biochemistry* **1996**, *35*, 9519.
72. Thomas, J. W.; Ellis, B.; Boerner, R. J.; Knight, W. B.; Wite, G. C., II; Shaller, M. D. *J. Biol. Chem.* **1998**, *273*, 577.
73. Alexandropoulos, K.; Baltimore, D. *Genes Dev.* **1996**, *10*, 1341.
74. Parang, K.; Kohn, J. A.; Saldahna, A.; Cole, P. A. *FEBS Lett.* **2002**, *26134*, 1.
75. Parang, K.; Cole, P. A. *Pharmacol. Ther.* **2002**, *93*, 1.
76. Parang, K.; Till, J. H.; Ablooglu, A. J.; Kohanski, R. A.; Hubbard, S. R.; Cole, P. *Nat. Struct. Biol.* **2001**, *8*, 37.
77. Lynch, B. A.; Loiacono, K. A.; Tiong, C. L.; Adams, S. E.; MacNeil, I. A. *Anal. Biochem.* **1997**, *247*, 77.
78. Waksman, G.; Kominos, D.; Robertson, S. C.; Pant, N.; Baltimore, D.; Birge, R. B.; Cowburn, D.; Hanfusa, H.; Majer, B. J.; Overduin, M.; Resh, M. D.; Rios, C. B.; Silverman, L.; Kuriyan, J. *Nature* **1992**, *358*, 646.
79. Payne, G.; Shoelson, S. E.; Gish, G. D.; Pawson, T.; Walsh, C. T. *Proc. Natl. Acad. Sci. U.S.A.* **1993**, *90*, 4902.